BIOLOGICAL EFFECTIVENESS OF COSMIC RAYS NEAR THE EARTH SURFACE

Belisheva N.K.
FGBUN Kola Science Centre Russian Academy of Science, Apatity, Russia

The earth is continually bombarded by high-energy particles that originate in outer space. These cosmic rays (CR) interact with the nuclei of atmospheric constituents, producing a cascade of interactions and secondary reaction products that contribute to CR exposures that decrease in intensity with depth in the atmosphere, from aircraft altitudes to ground level.

Primary cosmic particles are divided on galactic and solar origin. Galactic cosmic rays (GCR) incident on the top of the atmosphere consist of a nucleonic component, which in aggregate accounts for 98% of the total, and electrons, which account for the remaining 2%. The nucleonic component is primarily protons (88%) and alpha particles (11%), with the remainder heavier nuclei [1]. These primary cosmic particles have an energy spectrum that extends from 10^8 eV to over 10^{20} eV.

Another component of cosmic rays is generated near the surface of the sun by magnetic disturbances. These solar particle events are comprised mostly of protons of energies generally below 100 MeV and only rarely above 10 GeV (10^{10} eV). These particles can produce significant dose rates at high altitudes, but only the most energetic affect dose rates at ground level. Solar particle events can, in addition, disturb the earth's magnetic field in such away as to change the galactic particle intensity.

The only solar particle events of interest for radiation protection are those in which high-energy particles are produced that can increase ground-level radiation. The largest event yet observed occurred on 23 February 1956, during which the rates of neutron counts at ground level rose to 3600% above normal background levels [2].

The high-energy particles incident on the atmosphere interact with atoms and molecules in the air and generate a complex set of secondary charged and uncharged particles, including protons, neutrons, pions and lower-Z nuclei. The secondary nucleons in turn generate more nucleons, producing a nucleonic cascade in the atmosphere [3]. Because of their longer mean free path, neutrons dominate the nucleonic component at lower altitudes. As a result of the various interactions, the neutron energy distribution peaks between 50 and 500 MeV; a lower energy peak, around 1 MeV, is produced by nuclear deexcitation (evaporation). Both components are important in dose assessment.

Many measurements have been made of the altitude profile of the charged-particle and photon ionization and the absorbed dose rate in free air at ground level. The dose rate values may be considered as averages over the 11-year solar

activity cycle, with the total range of variation about 10%. Since mostly muons are involved, a radiation weighting factor of unity is appropriate [4], yielding the same values for the effective dose rate, i.e. 31nSv h^{-1} or 270 μSv a^{-1}.

It is much more difficult to estimate the neutron contribution to effective dose rate at sea level. Incoming protons that initiate the CR neutron field are strongly affected by the earth's magnetic field, with the effect that the neutron fluence rate in equatorial regions is less than that in polar regions. Investigators have recognized the importance of the latitude effect, but it has not been carefully quantified by reliable measurements. Florek et al. [5], quoting results of the Los Alamos LAHET code system calculation, suggest that the equatorial neutron fluence rate at sea level is one fifth the polar rate and that the rate at 50° latitude is 80% of the polar rate. Nakamura et al. [6], combining measurements made at Tokyo (24°N) with those for higher latitudes [7, 8], obtained a narrower range for the pole to equator variation, i.e. the equatorial rate about one fourth of the polar rate.

For both the directly ionizing and photon component and the neutron component of cosmic rays, there is a substantial altitude effect. For the directly ionizing and photon component the population-weighted average dose rate is 1.25 times that at sea level, and for neutrons 2.5 times. The population-weighted average value corresponds to the dose rate that occurs at 900 m above sea level. The calculations cited by Florek et al. [5] and the attenuation factor indicate that the effective dose rate from neutrons would increase by a factor of 2.1 between sea level and 900 m elevation. For the directly ionizing and photon component, the world average effective dose rate is 340 μSv a^{-1} (31 nSv h^{-1} or 270 μSv a^{-1} multiplied by the altitude factor of 1.25); for the neutron component, the average value is 120 μSv a^{-1} (48 μSv a^{-1} multiplied by the altitude factor of 2.5). These results apply to exposures outdoors [9].

So as CR are a natural source of ionizing radiation, the biological effects caused by the CR must comply with damages of genetic substance induced by ionizing radiation. The effectiveness of ionizing radiations to induce biological alterations depends on the way how the energy is deposited in the system. Densely ionizing radiations are more effective than photons or fast electrons the quantitative extent is given by the "relative biological effectiveness (RBE)" which is defined as the ratio of the doses to create the same effect by the reference radiation (commonly ^{60}Co-γ-radiation) and by the radiation in question. A common descriptor of radiation quality is "linear energy transfer" (LET), the energy locally imparted by a charged particle per unit distance traversed. LET is conceptually different from "stopping power" which stands for the energy lost by the incoming particle. LET does not take into account the microscopic structure of energy deposition and has, therefore, some limitations. RBE depends on LET but not in unambiguous manner as the same LET can be achieved by different ions depending on their charge and speed [10].

As it was demonstrated the densely ionizing (high linear-energy-transfer, LET) radiations, such as neutrons and a-particles, could have a greater biological effectiveness than sparsely ionizing (low-LET) X-rays or γ-rays [11, 12]. For many relevant effects in mammalian systems there is a general tendency to increasing RBE with increasing LET, up to a maximum (at ~100–200 keV μm^{-1} for a-particles) followed by a decrease at very high LET [10].

Direct mechanistic analysis of experimental data for neutrons or fast heavy ions are confounded by a variety of complications. For example, from fission neutrons the cell receives a very wide variety of tracks, mostly of recoil protons of energies about 0–10 MeV, LETs ~ 4–90 keVμm^{-1} and ranges about 0–1200 μm, including some tracks which stop, start, cross or are entirely internal to a cell nucleus. Furthermore, there is always a dose-component from accompanying low-LET γ-rays. Interpretation of effects from fast heavy ions is complicated by their long delta-ray electrons, which may travel across many cells (even millimetre distances) and irradiate them with essentially low-LET electrons. Mechanistic understanding of effects of neutrons should be aided by synthesis of understanding of the mechanisms of action of the charged particles in the recoil spectrum [10].

Damages of cellular DNA (or deoxyribonucleic acid, contained in cellular nuclei, Fig.1) arised under exposure of particles with high LET, are a main danger for cells. The nucleus of each cell contains approximately 1.8 meters of DNA in total, although each strand is less than one millionth of a centimeter thick. This DNA is tightly packed into structures called **chromosomes**, which consist of long chains of DNA and associated proteins. In eukaryotes (all organisms except viruses, Eubacteria and Archaea), DNA molecules are tightly wound around proteins – called **histone proteins** – which provide structural support and play a role in controlling the activities of the genes. A strand 150 to 200 nucleotides long is wrapped twice around a core of eight histone proteins to form a structure called a **nucleosome.** Each chromosome has a **p arm** and a **q arm**. The p arm is the short arm, and the q arm is the long arm. In their replicated form, each chromosome consists of two **chromatids [**13].

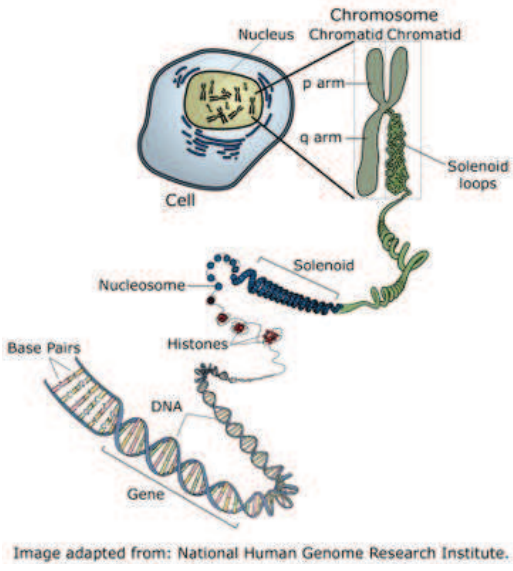

Fig. 1.

A high-LET track is more likely to damage a cellular structures than a single low-LET track. However, on the basis of equal absorbed dose (approximately equal average numbers of ionizations per unit volume), there are two competing trends. The small numbers of high-LET tracks per unit dose (approximately proportional to 1/LET) are less likely to pass through any given target or micro-

scopic region of the cell, but if they do they are more likely to cause substantial damage. On this basis alone it is not obvious *a priori* whether 1 α-particle would be more biologically damaging to the DNA of a cell than would several hundred electrons, for a similar dose to the cell nucleus. High-LET-track correlations are apparent at all of levels of tissue, cellular, nuclear organizations [14]. It is believed that intense fluxes of secondary cosmic rays, which include particles with high LET radiation could cause lesions at the cellular level, similar to disorders induced by ionizing radiation with high-LET and with low-LET tracks.

Our studies were performed during a great solar proton events with Ground Level Enhancements (GLE) in the secondary cosmic rays, detected by ground based neutron monitor (Polar Geophysical Institute, Neutron monitor station at Apatity). The year 1989 has manifested an exceptionally large number of sunspots and solar flares, energetic particle events in the near-Earth space environment, and ground level neutron enhancements. Three very energetic solar proton events (SPE) were observed during the period of 19–31 (GLE 43, GLE 44, GLE 45) October 1989 on board geosynchronous satellites GOES 6 and GOES 7. In each case, ground based neutron monitors have detected exceptionally high neutron intensity increases.

The aim of this report is demonstration of the experimental evidence of ground-based radiation effects in biological systems induced by CR.

Biological effects of a Great Solar proton events in October 1989

Six separate biological experiments were conducted on 15–31 October 1989 (Fig. 2) on three cellular lines growing in cultures: At the beginning of each experiment, cellular monolayers from the culture flasks were dispersed and a single cell suspension in culture medium were inoculated into the antibiotic flask in quantity of 50 000 cells, where cells adhered to the surface of the cover glasses. During the period of cell cultivation on the cover glasses, 3–5 samples of antibiotic flasks for each cell lines, in each experiment, every 3, 6, and 12 h were selected for fixation of cells (Fig. 3). Before cell fixation, 1 μKu/ml of ^{3}H-thymidine was added for 30 min for far visualization of nuclei with DNA synthesizing activity. The glasses with adhering cells marked by the ^{3}H-thymidine, were covered by a photo-emulsion (Ilford), were kept for three months in the dark, were developed, were stained with hematoxilin-eosin, and were then made permanent preparations for far analysis. Permanent preparations were analyzed by epi-fluorescence microscope Zeiss Axioskop 2, coupled with image device and software for image analysis (Media Cybernetics, Inc.). Cells with single nuclei, with gigantic nuclear, with micro nuclear, and with multinuclear cells (MNC) were counted with the microscope by using 10–20 fields of view. The morphofunctional dynamics were estimated by index of MNC (percentage of MNC in the cell population normalized against the mean MNC during the quiet period (15–18 October 1989). For analysis of morphofunctional dynamics, the

indices of MNC in six separated experiments were averaged on coinciding time serious points for each cellular line.

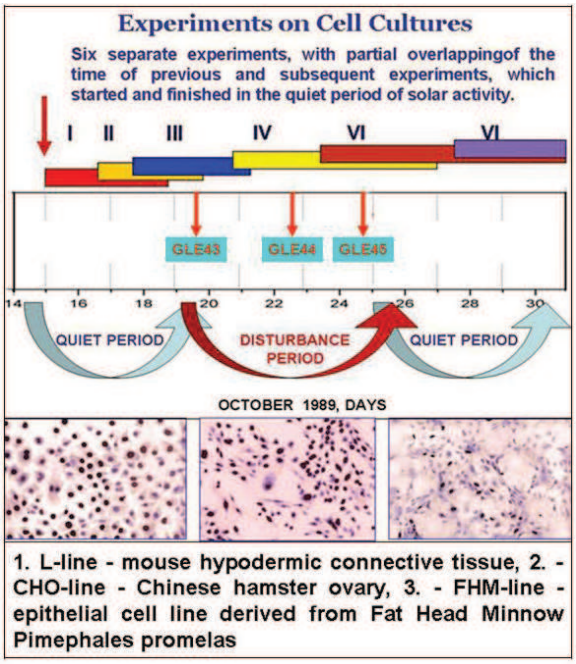

Fig. 2.

The data on solar activity and high energetic particles were downloaded from the site http://spidr.ngdc.noaa.gov/spidr/. Ground-based neutron monitor data were provided by the station of neutron monitor of the Polar Geophysical Institute (PGI), KSC RAS in Apatity (67.34ºN, 33.24ºE). The Monte Carlo PLANETOCOSMICS code based on GEANT4 [16] has been used for calculation of particle cascades in the atmosphere during SPE, associating with Ground Level Enhancements (GLE43, GLE 44, GLE45). The representation of physical properties of the atmo sphere was realized by the NRLMSISE-00 model. The source of primary protons with the given energy distribution (0,5–10 GeV) on boundary of the atmosphere (80 km) has been used in calculation of secondary solar particle generation (data of E. Maurchev). The solar proton data (GOES 6, GOES 7), the long-term balloon measurements, ground-based neutron monitors observations were selected to calculate the particle fluxes on the level of Apatity (950 g/cm^2) for GLEs events in October 1989. Resulting fluxes were obtained, as integral [16]. Ambient and Personal Dose equivalent per Unit Neutron Fluence, $H^*(10)/\Phi$ was applied for calculation neutron doses [15]. According to Summary of recommended radiation weighting factors and Q–L relationships the neutron spectrum was shared on energy ranges in correspondence to quantities of weighting factors [15].

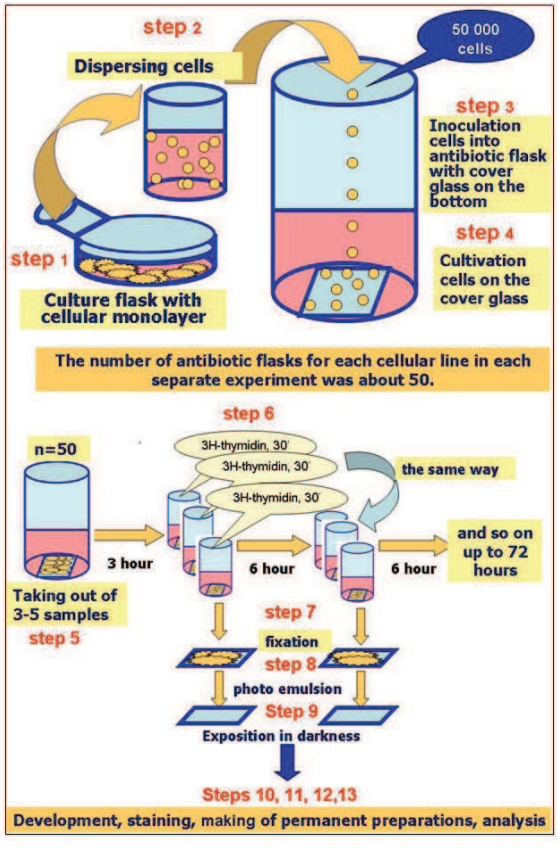

Fig. 3.

Extraordinary phenomena (Fig. 4) were detected in the morphofunctional state of three different cellular cultures during performed experiments [17].

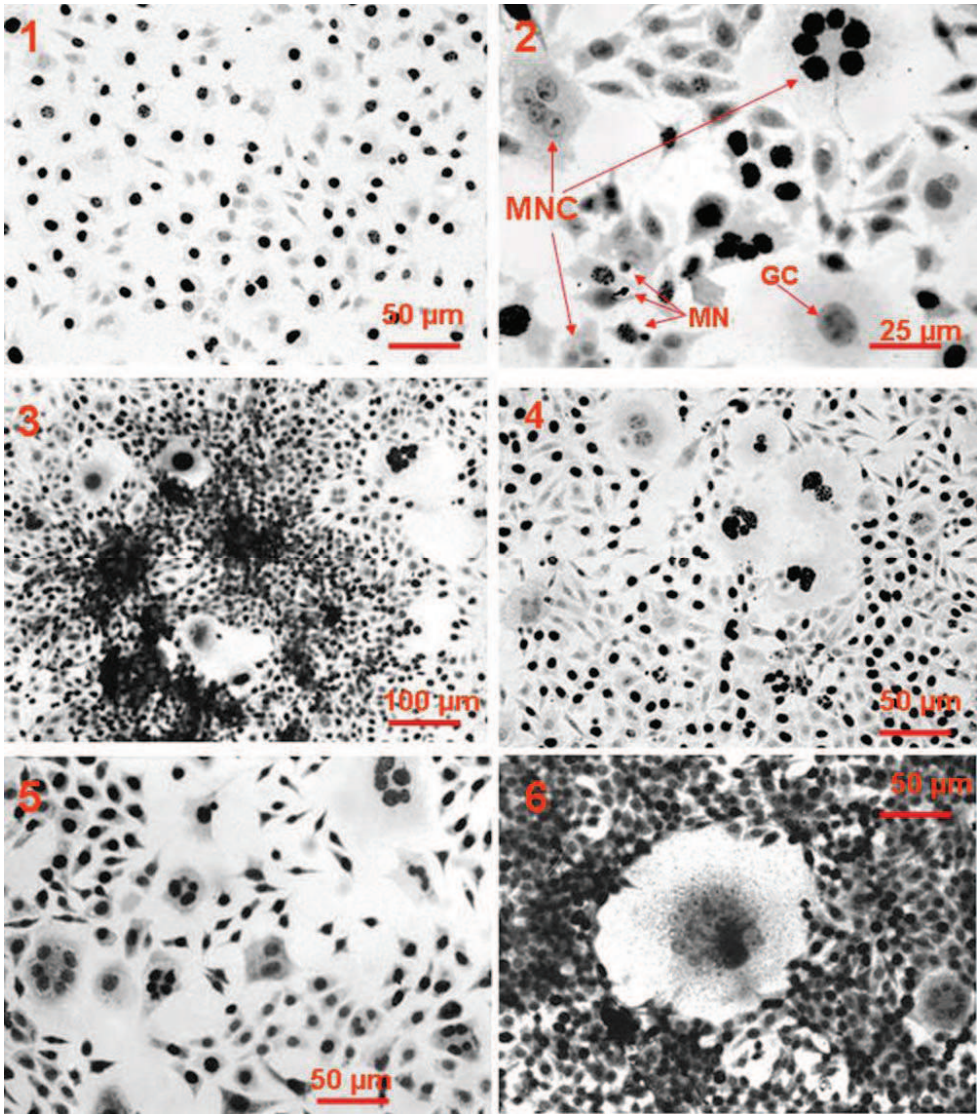

Fig. 4.

In Figure 4 are shown the state of cellular culture L-line in quiet period (15–18 October 1989), (1) and during CLEs (19–25 October 1989) (2–6). Phenomena in state cellular cultures during GLEs were manifested as an abrupt increase of multinuclear cells (MNC), Fig. 4(2–6); gigantic cells (GC), Fig.4 (2–6); multiple disorders of cellular and nuclear substances, including the appearance of cells with apoptosis (Fig. 4(4,6)) and micronuclei (Fig. 4(2,5)); local region of clustered damages (Fig. 4(3–6)); coherent manifestation of signatures (2-6) in the three lines (Fig. 5).

Some of damages were typical under exposure of ionizing radiation on the cells: MNC, GC, apoptosis, micronuclei (including a small region of clustered damages [18–24] Clustered damages of nuclear substances were similar to the

"bystander" responses, involving damage to the nearby cells that were not directly traversed by the radiation [12, 14, 20, 23, 25].

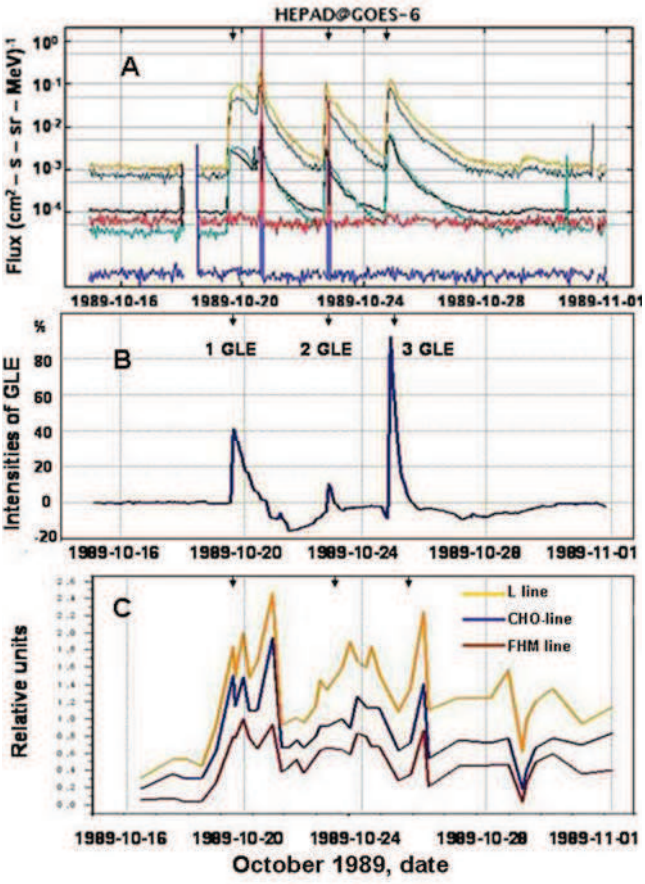

Fig. 5.

Dynamics of MNC indices have revealed synchronous appearances of DNA damages and identical types of lesions in three cellular lines (Fig. 5). Timing of the dynamics of the MNC-indices (Fig. 5, C), the arrival of fluxes of solar energetic particles detected by the GOES-6 satellite in the Earth's orbit (Fig. 5, A), and data obtained by the ground-based neutron monitor (Fig. 5, B), show that the increase of the intensity of ionizing radiation on the Earth's surface in association with solar proton events are additional evidence for a cause-effect relation between solar energetic particles and the revealed phenomena. The first arrival of most energetic particles, which produce a dramatic hardening of the spectrum but not much change in the flux [26] is apparent in the correlation coefficients between the MNC indices, protons with energies >850MeV, and neutron count rate [17]. "The three GLEs observed in October 1989 correspond very well with the three main flux onsets and increases in spectrum hardness" [26]. The second arrival (Fig. 5) of more plentiful but lower energy particles dramatically increases the flux [26] is not detected by the neutron monitors, however damages in the cellular line were induced by lower energy particles than during first arrival of most energetic particles. Thus, the cellular and nuclear disorders could be induced by a cascade of secondary particles, which are generated in the upper atmosphere by solar energetic particles with both hard and softer spectra and are able to achieve the Earth's surface.

The CRs near the Earth's surface are presented by secondary particles, where more than 97% of hadronic component are neutrons at sea level [27]. Neutrons under interaction with matter produce the recoiling nucleus (charged proton), which is the source of ionizing events. The low-energy protons form densely ionizing tracks (high LET) which are efficient in producing biological injury. Differential energetic neutron fluxes at the depth of the atmosphere 950 g/cm^2 have been selected to calculate the neutron fluencies during GLE 43, GLE 44, GLE 45 (Figure 6). Two-component structure of increase of high energy par-

ticles were detected in solar proton intensity associated with GLE 43, 44, 45. A peak of a short fast (fc) component with following peak of a delayed (dc) component was found during increase of proton intensity in these solar events. Neutron fluxes generated by fast (fc) and by delayed (dc) components of solar protons were separately considered in this research. Differential particle fluxes for the three cases GLE (43, 44, 45) generated by fast and delay compo-nents with different RBE expressed across weighting factors (Wr) which correspond to LET are demonstrated in Figure 6. Neutron fluxes generated by fast (A) and delay (B) components of solar particles on latitude of Apatity (67.57° N, 33.40° E, 0.65 GV, 950 g/cm^2); Wr–weighting factors corresponding of neutron energy range RBE; LET (keV per micron) of certain neutron energy ranges are shown in the Figure 6.

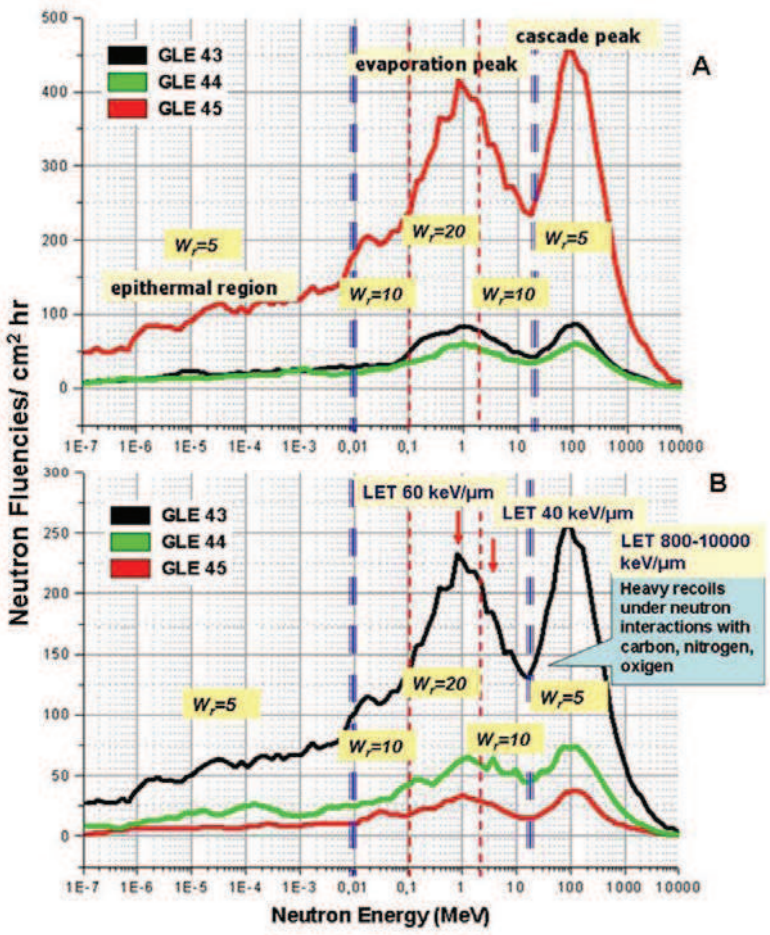

Fig. 6.

Table 1 demonstrates correspondence of a certain types and energy ranges to Radiation weighting factors [15].

The neutron fluencies calculated for fast and for delay components of three GLEs were divided on energy ranges according to type and energy range in Table 1. (Figure 7, A): fast components – red and delay components – blue columns. Separated doses from contributions by fast (red) and by delay (blue) components of neutron energy ranges were assessed according to [15], Figure 7, B. demonstrates contributions of the neutron fluxes with certain energy range from fast and delayed components of solar protons to the Ambient Dose Equivalent per unit neutron fluence, $H^*(10)/\Phi$(pSv cm^2 hr). Abscise: 1.< 10 ke V, *Wr* = 5; 2.10 keV to 100 keV, *Wr* = 10; 3 .> 100 keV to 2 MeV, *Wr* = 20; 4. > 2 MeV to 20 MeV *Wr* = 10; 5. > 20 MeV, *Wr* = 5; 6. Total Fluence (fast and delay components) (A), total doses of fast and delayed components (B). Ordinate: Neutron density fluxes (neutrons/cm^2 hr).

Table 1.

Type and energy range	Radiation weighting factor
Photons, all energies	1
Electrons and muons[a], all energies[b]	1
Neutrons, energy:	
< 10 keV	5
10–100 keV	10
0.1–2 MeV	20
2–20 MeV	10
> 20 MeV	5
Protons, other than recoil protons, energy > 2 MeV	5
α-particles, fission fragments, heavy nuclei	20

One can see in Figure 9, that neutron fluxes beginning from energy range > 100 keV to 2 MeV (Wr = 20) make a significant contribution to Ambient Dose Equivalent per unit neutron fluence in three GLEs. And, if the primary contribution to the Ambient Dose Equivalent in GLE 43 was made by delay component (blue color, Fig.7), so as in GLE 44, the main contribution to Ambient Dose Equivalent in GLE 45 was contributed by fast component (red color, Fig. 7). By the fact that fast component in GLE 45 had a most hard spectrum, the maximum bio effective-ness of solar proton events was revealed during GLE 45. The data obtained from the analysis of cellular culture state during three cases of GLEs shown the maximum alterations in cellular cultures during GLE 45.

The fragmentation of chromatin (dispersion of DNA), the damage of nucleosomes with their further lysis, a manifestation of super fluidity DNA detectable by merging of the contents of the nuclei in a few cells, multiple tracks from charged particles traversing through the cell monolayer during GLE were found in the cellular cultures. Some of these effects, induced by secondary particles of solar proton events in cellular cultures are shown in Figures 8, 9.

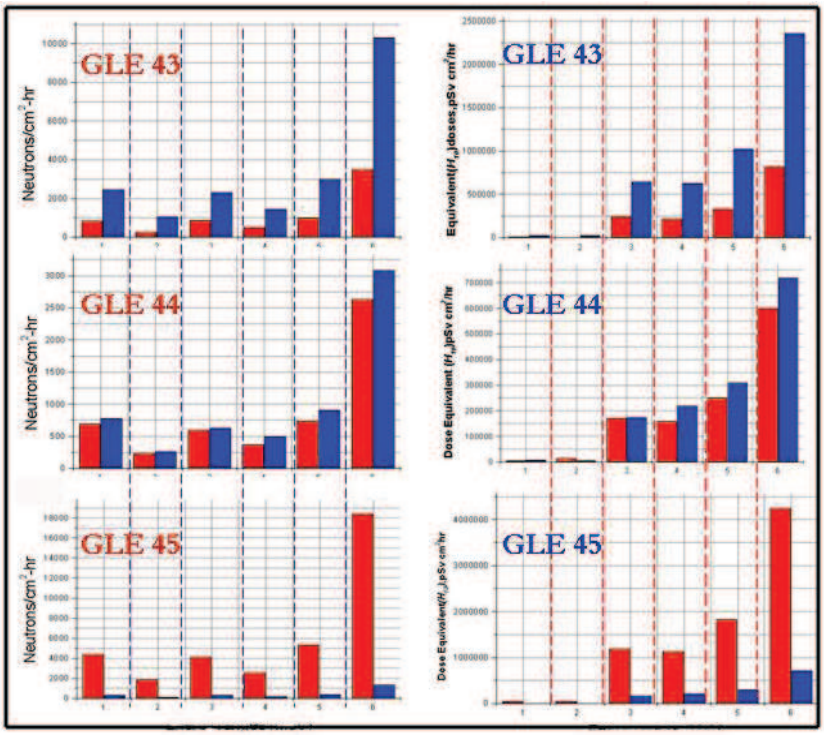

Fig. 7.

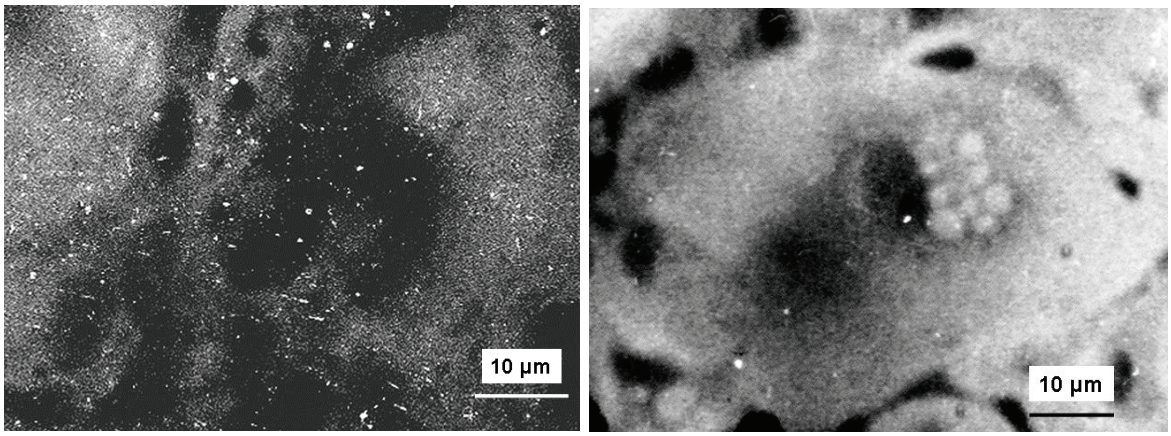

A B

Fig. 8.

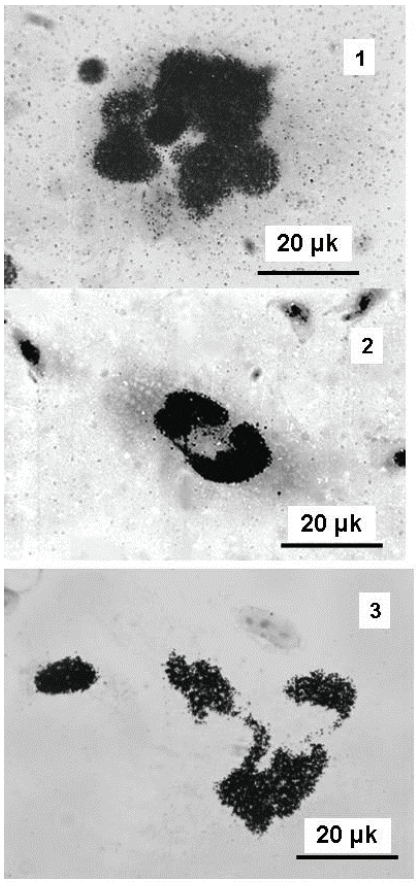

DNA damages: 1 L-line, 2- CHO line, 3- FHM line

Fig. 9.

Practically the all structures of cellular nuclei shown in Figure 1 were damaged in the cells which were traversed by charged particles. Figure 8 shows tracks from charged particles in cellular culture FHM line during GLE 45. Holes in nuclei (A) and denaturation of DNA strands with release of energy at the peak of Bragg (evaporation of water in the end of particle way) one can see in Figure 8, (B).

Figure 9 demonstrates diverse DNA damages in the L line (1), CHO line (2), FHM line (3). Multiple DNA damages in cellular cultures during the solar proton events in October 1989 associated with increase of the neutron intensity near the Earth surface are result of the passage of energetic photons, electrons and ions which produces a track of ionized and excited atoms and molecules within the irradiated matter.

Presented data is evidence of high effectiveness of the secondary solar cosmic rays during GLEs. Comparison of the tracks from secondary particles in the own experimental data with images of tracks from heavy charged ions traversing through single cellular nucleus [22] demonstrated the similarity between exposure of charged particles on the cells in experiments [22] and exposure of secondary cosmic rays on biological objects. Hence one be suggested that particles with high LET radiation, fragments and recoils, as well as the neutrons generated in the nuclear cascade during GLEs could be responsible for the diverse phenomena observed in the cell cultures near the Earth's surface.

Sum fluxes and doses from three GLEs are presented in Table 2. Total fluxes (fc+dc) during GLE 43, 44, 45 were estimated as 13801.7, 5714.1, 19807.1 n/cm^2-hr. The summary calculation gives previous estimations of number of particles and ambient dose equivalent during GLE's events: near the 40 000 neutrons in the all energy range per hour have passed through the every cellular monolayer during three GLE events. It is mean, that in average, every second cell were passed by one or several particles. The integral ambient dose equivalent from three cases of GLE consists of about 217 μSv per three days. This is almost half of daily doses which were measured on the board of space stations 535 μSv/day [28] and more than average annual *Effective dose rate (μSv a^{-1})* under outdoors, altitude adjusted conditions exposure of neutrons (124 μSv a^{-1}).

Table 2.

GLE 43, October 19, 1989	fc+dc n/ cm^2-h	microSv cm^2/h	microSv cm^2/day
>100keV-2 MeV	3196,553	0,892439	21,41854
2-20 MeV	1971,491	0,855875	20,54101
>20 MeV	3986,709	1,359558	32,6294
Total Flux/dose	13801,7	3,172976	76,15142
GLE 44, October 22, 1989			
>100keV-2 MeV	1222,858	0,345826	8,299832
2-20 MeV	870,4813	0,379227	9,10144
>20 MeV	1647,177	0,560509	13,45223
Total Flux/dose	5714,104	1,319835	31,67604
GLE 45, October 24, 1989			
>100keV-2 MeV	4463,907	1,279829	30,71591
2-20 MeV	2792,778	1,20574	28,93775
>20 MeV	5785,201	1,974703	47,39288
Total Flux/dose	19807,1	4,559667	109,432

Effects of daily variations of cosmic rays in ground-based experiments

We have shown that the regular solar-daily variations of cosmic rays and the sporadic increase of their intensity are associated with fluctuations of MNC indices reflecting the dynamics of cellular fusion [29] The studies were performed with continuous cell lines growing *in vitro* : CHO line; FHM line; and RTG line- the rainbow trout (*Salmo gairdneri*) gonad-cells. A comparison of the state of cellular cultures of different origin (fish and hamster) growing under similar conditions, and identical cultures growing under different conditions (at

37° and at 20°) allows identifying universal cellular response on hit of the secondary cosmic rays into cells. The dynamics of cellular culture state were estimated by index of MNC (percentage of MNC in the cellular population).

In the course of the analysis of cellular functional state the multiple lesions associated with cellular nuclear were found. Binuclear cells (BNC), cells with gigantic nuclei (GN), apoptosis (Ap), micronuclei, holes in the distorted cells were revealed (Figure 10). In Figure 10 arrows show the multiple lesions and

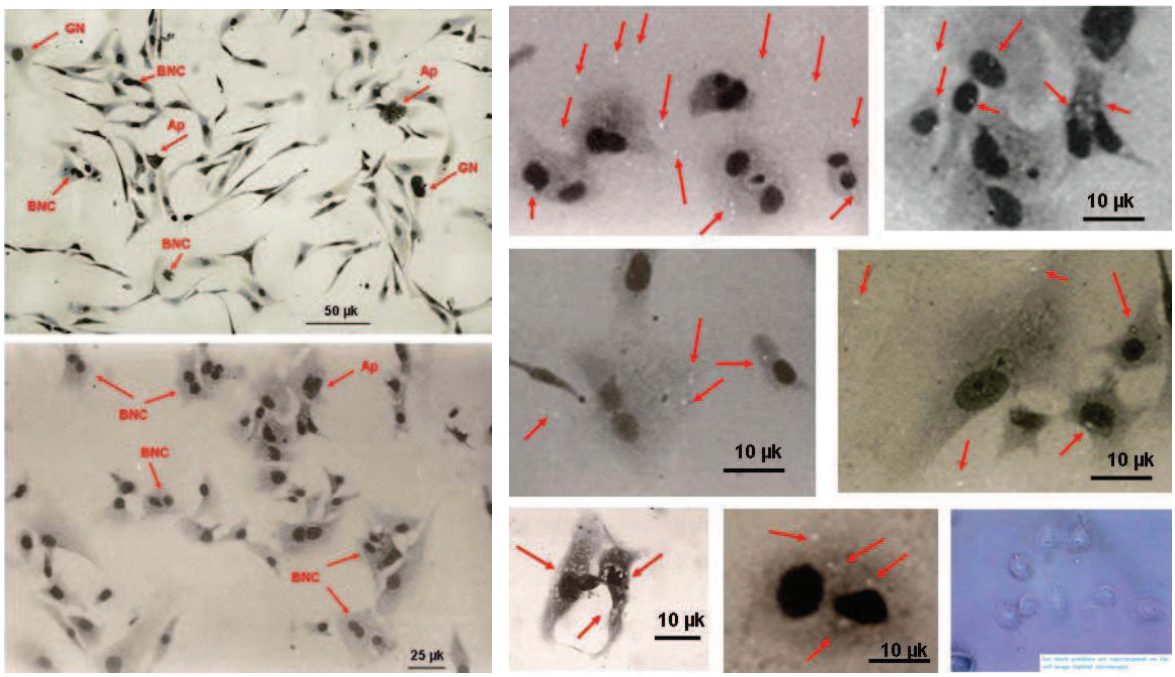

Fig. 10.

“holes” in cellular culture of RTG line. Holes are similar with track of heavy charge particles traversing the cellular samples in the space experiments (blue image in the right corner). Concordance between variations of neutron intensity and dynamics of indices MNC, lesions in cellular nuclei, holes in the cells and cellular environment are evidence of the passage of energetic photons, electrons and ions which produces a track of ionized and excited atoms and molecules within the irradiated matter. Charged particles in the composition of the secondary cosmic rays are detected by tracks arising in result of traversing particles through cellular monolayer.

Figure 11 shows the simultaneous changes in the variations of neutron intensity near the Earth surface and in the dynamics of MNC indices reflecting the cell fusion in the tested cellular lines. The variations in the neutron count rate intensity (Fig. 11; 1) and in the indices of MNC in cellular cultures: (2) CHO line and (3) RTG line growing at 37°C and (4) RTG line growing at room temperature (20°C) on August 19–22 (top picture) and October 12–17, 1990 (bottom picture). The abscissa shows the numbers of corresponding to the dates of experiments: (top picture) August 19 (*1*,*2*,*3*), August 20 (*4*,*5*,*6*), August 21 (*7*,*8*),and

August 22 (*9*,*10*); (bottom picture) October 12 (*1*,*2*,*3*), October 13 (*4*), October 15 (*5*,*6*), October 16 (*7*,*8*), and October 17 (*9*).

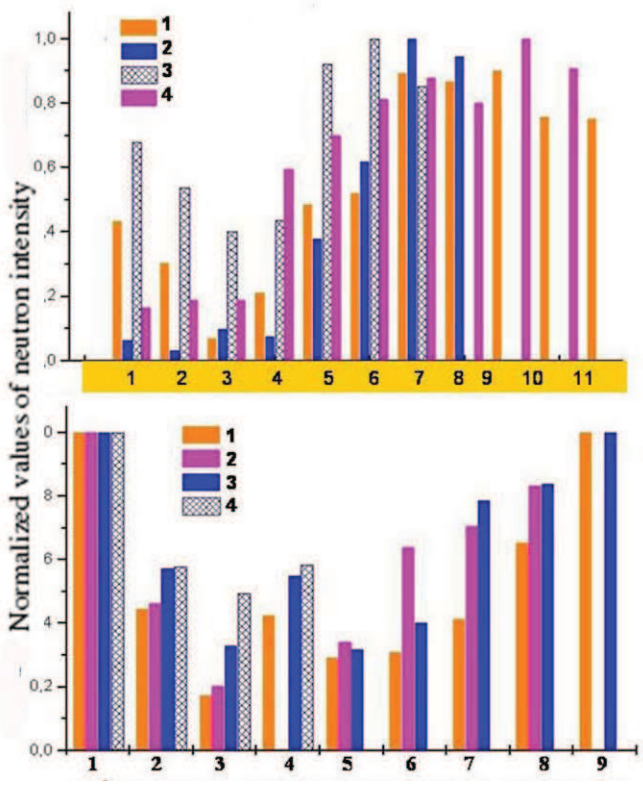

Fig 11.

Thus, we discovered that variations in the intensity of the neutron component of cosmic rays near the earth's surface are accompanied by biological phenomena, which manifests itself as cell fusion in cell cultures. Synchronous cell fusion in the all cell lines irrespective of their origin and culturing conditions is indicative about similar response of cell systems on the exposure of background variations of the neutron component, which may be represented by neutrons of different energy ranges including the neutrons with high LET and high RBE. One can suppose that the tracks from charged particles traversing through cells and cellular nuclei induce cellular fusion.

Conclusions

The direct evidence of effects of CR on biological systems is presented in this report. This evidence has been obtained in the experiments on three cellular lines growing in vitro during solar proton events (SPE) accompanied by three cases of GLEs in October 1989.

Diverse phenomena associated with DNA lesions were found on the three cellular lines: tracks from charged particles traversing through cells, disorders of nuclei, multinuclear cells and cells with gigantic nuclei, micronuclei, apoptosis and other lesions. These disorders one can consider as result of the hit of charged particles from secondary solar cosmic rays in cellular targets.

The dynamics of the formation of multinuclear cells was simultaneous in the three cellular lines, the curves of dynamics coincident with the profiles of solar energetic particles arriving at near Earth space, and the main peaks in the number of multinuclear cells coincident with three cases of GLEs detected by a ground based neutron monitor.

The secondary solar cosmic particles near the Earth surface during GLE events in October 1989 have generated the cascades of ions, including the heavy charge ions and nuclear recoils. These secondaries corresponded to products of

nuclear interactions between fast neutrons and biological matter in the energetic range of the evaporation and the cascade peaks.

The total neutron fluxes during GLEs were calculated on the base of simulation of the particle cascades in the atmosphere by using of the Monte Carlo PLANETOCOSMICS (code GEANT4). Calculation of neutron fluxes gives preliminary estimations of number of particles and ambient dose equivalent during GLE's events (217 μSv cm2 per three days) that is almost half of daily doses which were measured on the board of space stations 535 μSv/day [28] and more than average annual Effective dose rate (μSv a-1) under outdoors, altitude adjusted conditions of exposure of neutrons (124 μSv a-1) [9].

The disorders of genetic matter in the three cellular lines, neutron fluxes and ambient dose equivalent are direct evidence of high biological effectiveness of the solar proton events in October 1989.

The degree of expressions of found lesions depend on the intensity of neutron component of the secondary cosmic rays near the Earth's surface.

The tracks from particles traversing through biological objects are evidence that charge particles may be responsible for lesions in the different cells.

Synchronous cell fusion in the all cell lines irrespective of their origin and culturing conditions is indicative of the similar response of cell systems to background variations of the neutron component, which may be represented by neutrons of different energy ranges including the neutrons with high LET and high RBE.

The results of the ground-based experiments on cellular cultures demonstrated the high biological effectiveness of the secondary cosmic rays.

References

1. *Gaisser, T.K.* Cosmic Rays and Particle Physics. Cambridge University Press, Cambridge, 1990.
2. *Shea, M.F. and Smart, D.F.* History of solar proton event observations, in: Proc. Suppl. Nuclear Physics B, 39, 16–25, 1995.
3. *Allkofer O.C., P.K.F. Grieder.* Fachinformationszentrum Energie, Physik, Mathematik, 1984 – 379 p.
4. International Commission on Radiological Protection. 1990 Recommendations of the International Commission on Radiological Protection. Annals of the ICRP 21(1–3). ICRP Publication 60. Pergamon Press, Oxford, 1991.
5. *Florek, M., J. Masarik, I. Szarka et al.* Natural neutron fluence rate and the equivalent dose in localities with different elevation and latitude. Radiat. Prot. Dosim. 67(3): 187–192 (1996).
6. *Nakamura, T., Y. Uwamino and T. Ohkubo.* Altitude variation of cosmic-ray neutrons. Health Phys. 53(5): 509-517 (1987).
7. *Hajnal, F., J.E. McLaughlin, M.S. Weinstein et al.* 1970 sea-level cosmic-ray neutron measurements. HASL-241 (1971).
8. *Hewitt, J.E., L. Hughes, J.B. McCaslin et al.* Exposure to cosmic-ray neutrons at commercial jet aircraft altitudes. p. 855–881 in: Natural Radiation Environment III, Volume 2. CONF-780422 (1980).

9. United Nations. Sources and Effects of Radiation. Vol. I: Sources; Vo. II: United Nations Scientific Committee on of Atomic Radiation, 2000 Report to the Assembly, with scientific annexes: ANNEX B. Exposures from natural radiation sources (156 p.) United sales publications E.00.IX.3 and Nations, New York, 2000.
10. *Kiefer Jü.* The physical basis for the biological action of heavy ions// New J. Phys. 10 (2008) 075004. doi:10.1088/1367-2630/10/7/075004
11. *Sverdlov, A.G.* Biologic Action of Neutrons and Chemical Protection, Nauka, Leningrad, 223, 1974.
12. *Akoev, I.G. and Yurov, S.S.* The results of biological experiments in space and biophysical interpretation of hadronic effects, in: Questions of biological effects and dosimetry of heavy charged particles and high-energy hadrons, edited by: I.G. Akoev, Puschino Scientific Center, 126–143, 1984.
13. http://www2.le.ac.uk/departments/genetics/vgec/schoolscolleges/topics/dna-genes-chromosomes
14. *Goodhead D.T.* Mechanisms for the Biological Effectiveness of High-LET Radiations// J. Radiat. Res., 40: SUPPL., 1–13 (1999).
15. IAEA Safety Standards Series. Assessment of Occupational Exposure Due to External Sources of Radiation. Safety Guide. No. RS-G-1.3. IAEA. Venna. 1999. 89 p.
16. *Maurchev E.A., Yu.V. Balabin, E.V. Vashenyuk and B.B. Gvozdevsky.* Transport of solar protons through the atmosphere during GLE // 2013 J. Phys.: Conf. Ser. **409** 012200 doi:10.1088/1742-6596/409/1/012200
17. *Belisheva N.K., H. Lammer, H.K. Biernat, and E.V. Vashenuyk.* The effect of cosmic rays on biological systems – an investigation during GLE events// Astrophys. Space Sci. Trans., 8, 7–17, 2012 www.astrophys-space-sci-trans.net/8/7/2012/
18. *Holley, W.R. and Chatterjee, A.* Clusters of DNA Damage Induced by Ionizing Radiation: Formation of Short DNA Fragments. I. Theoretical Modeling.// Radiat. Res. 145, 188–199 (1996).
19. *Nikjo H., I.P. O'Neill, W.E. Wilson and D.T. Goodhead.* Computational Approach for Determining the Spectrum of DNA Damage Induced by Ionizing Radiation// RADIATION RESEARCH 156, 577–583 (2001).
20. *Hall E.J, and T.K Hei.* Genomic instability and bystander effects induced by high-LET radiation// Oncogene (2003) 22, 7034–7042.
21. *Goodhead D.T.* Enegy deposition stochastics and track structure: what about the target?// Radiation Protection Dosimetry (2006), Vol. 122, No. 1–4, pp. 3–15. doi:10.1093/rpd/ncl498 Advance Access publication 2 February 2007.
22. *Jakob B., J. Splinter, M. Durante, and G. Taucher-Scholz.* Live cell microscopy analysis of radiation-induced DNA double-strand break motion // PNAS, 2009, March 3, vol. 106, no. 9, P. 3172–3177.
23. *Friedland W., Michael Dingfelder, Pavel Kundrát, Peter Jacob.* Track structures, DNA targets and radiation effects in the biophysical Monte Carlo simulation code PARTRAC//Mutation Research 711 (2011) 28–40.
24. *Alloni D., A. Campa, W. Friedland, L. Mariotti & A. Ottolenghi.* Track structure, radiation quality and initial radiobiological events: Considerations based on the PARTRAC code experience// International Journal of Radiation Biology, January–February 2012; 88(1–2): 77–86.
25. IARC Monographs on the evaluation of carcinogenic risk to human. Ionizing Radiation, Part 1:X- and Gamma (γ)-Radiation, and Neutrons. Vol. 75 Lyon, 26 May–2 June 1999. 2000.
26. *Reeves, G.D., Cayton, T.E., Gary, S.P., and Belian, R.D*. The great solar energetic particle events of 1989. Observed from geosynchronous orbit, J. Geophys. Res., 97, 6219–6226, 1992.

27. *Ziegler, J.F.* Terrestrial cosmic rays, IBM, J. Res. Develop., 40,19–39, 1996.
28. *Reitz G., R. Beaujean, E. Benton, S. Burmeister, Ts. Dachev, S. Deme, M. Luszik-Bhadra and P. Olko.* Space radiation measurements on – board ISS – THE DOSMAP EXPERIMENT//Radiation Protection Dosimetry (2005), Vol. 116, No. 1–4, pp. 374–379.
29. *Belisheva N.K., B.M. Kuzhevskii, E.V. Vashenyuk, and V.K. Zhirov.* Correlation between the Fusion Dynamics of Cells Growing in vitro and Variations of Neutron Intensity near the Earth's Surface. Doklady Biochemistry and Biophysics. 2005. V. 402. P. 254–257.

Summary

A direct evidence of biological effects of cosmic rays (CR) near the Earth surface was demonstrated in experiments with three cellular lines growing in culture during three events of Ground Level Enhancement (GLEs 43,44,45) in the neutron count rate detected by ground-based neutron monitor in October 1989 and during a quiet period in August, October 1990. Time coincidence of numerous disorders of nuclear substances in three cell lines with solar proton events and Ground Level Enhancement gives the basis to consider the increase of secondary components of solar cosmic rays as a reason of revealed phenomena. The simulation of particle cascades in the atmosphere by using the Monte Carlo PLANETOCOSMICS code based on GEANT4, solar proton data (GOES 6, GOES 7), ground-based neutron monitors observations were used for calculation of particle fluencies at the latitude of the Apatity (67.57 N, 33.40 E, 0.65 GV, 950 g/cm^2). Neutron fluxes generated by fast (fc) and by delayed (dc) components of solar particles in three events were taken for consideration. The drastic increase of neutron fluencies near the Earth surface at the Apatity latitude was found during three GLEs. Total fluxes (fc+dc) during GLE 43, 44, 45 were estimated as 13801.7, 5714.1, 19807.1 n/cm^2-hr. The integral ambient dose equivalent from three cases of GLE consists of about 217 μSv per three days, that is almost half of daily doses on the board of space stations 535 μSv/day and more than average annual effective dose rate under outdoors, altitude adjusted conditions exposure of neutrons (124 μSv a^{-1}). Synchronous cell fusion in the all cellular lines irrespective of their origin and culturing conditions during quiet period in August and October 1990 confirms the high biological effectiveness of the secondary cosmic rays.